



Photoreactivity of chromophoric dissolved organic matter transported by the Mackenzie River to the Beaufort Sea

Christopher L. Osburn^{a,*}, Leira Retamal^b, Warwick F. Vincent^b

^a Department of Marine, Earth, and Atmospheric Sciences, North Carolina State University, 2800 Faucette Drive, Raleigh, NC, 27695, USA

^b Département de biologie & Centre for Northern Studies (CEN), Laval University, Quebec City, QC, Canada G1V 0A6

ARTICLE INFO

Article history:

Received 18 November 2008
Received in revised form 11 May 2009
Accepted 11 May 2009
Available online 18 May 2009

Keywords:

Chromophoric dissolved organic matter
Dissolved organic carbon
Photodegradation
Mackenzie River
Arctic Ocean

ABSTRACT

The photoreactivity of chromophoric dissolved organic matter (CDOM) transported to Arctic shelf environments by rivers has only recently been studied and its quantitative role in Arctic shelf biogeochemistry has received little attention. Sunlight exposure experiments were performed on CDOM collected over a three year period (2002 to 2004) from river, estuary, shelf, and gulf regions of the Western Canadian Arctic. Decreases in CDOM absorption, synchronous fluorescence (SF), and dissolved organic carbon (DOC) concentration were followed after 3 days of exposure, and in two experiments, six optical cutoff filters were used to incrementally remove ultraviolet radiation incident on the samples. Apparent quantum yields for CDOM photobleaching (AQY_{ble}) and for DOC photomineralization (AQY_{min}) were computed, as were two AQY spectra (ϕ_{ble} and ϕ_{min}) for the Mackenzie River and a sample from the Mackenzie Shelf. The photoreactivity of Mackenzie River CDOM was highest after break-up and peak discharge and lowest in late summer. The half-lives of CDOM and DOC were estimated at 3.7 days and 4.8 days, respectively, when Mackenzie River water was exposed to full sunlight. Photobleaching of Mackenzie River CDOM fluorescence after most UV-B wavelengths were removed increased the correlation between the river and offshore waters in the Beaufort Sea. When light attenuation from particle- and CDOM-rich river water was considered for the Mackenzie Shelf, our photodegradation models estimated around 10% loss of absorption and < 1% DOC loss, suggesting that sunlight exposure does not substantially degrade CDOM on Arctic shelves.

© 2009 Elsevier B.V. All rights reserved.

1. Introduction

Climatic warming in the Arctic can result in the loss of sea ice and an increased riverine discharge to the surface waters of the Arctic Ocean (Peterson et al., 2006). With increased riverine flow, fluxes of terrigenous dissolved organic matter (DOM) can also increase (Dixon et al., 1994; Oelke et al., 2004). Given the proximity to large rivers, most DOM on Arctic shelves originates from terrigenous sources and is transported in river discharge.

The Mackenzie River is the 4th largest freshwater discharge and the largest source of particulates to the Arctic Ocean (Macdonald et al., 1998), dominating the western Arctic region of Beaufort Sea. Seasonal discharge historically increases after break-up in early May, when the river floods its extensive delta, and then decreases during a recession period throughout the summer (Emmerton et al., 2008). Thus river flow is largest in the late spring–early summer and lowest in the winter when much of the river remains frozen. The flux of DOM from this river to the Beaufort Sea is linked to its hydrology and thus varies considerably (Emmerton et al., 2008). Only recently has the DOM of

this river been studied (Droppo et al., 1998; Retamal et al., 2007; Emmerton et al., 2008).

Terrigenous DOM strongly absorbs sunlight. The ultraviolet and visible light absorption by this chromophoric dissolved organic matter (CDOM), in addition to particulate matter, controls and structures the euphotic zones in the coastal waters of the Arctic shelves. Two important biogeochemical consequences that can result from CDOM light absorption are investigated here: the photomineralization of organic C to inorganic C (Mopper and Kieber, 2002) and photobleaching (Del Vecchio and Blough, 2002; Osburn and Morris, 2003). Photomineralization represents a source of CO₂ to the atmosphere whereas photobleaching can increase the relative depth of the euphotic zone to the mixing zone in surface waters (Del Vecchio and Blough, 2002). Photobleaching can increase the penetration of UV radiation as well as photosynthetically available radiation (PAR) into the water column, with a combination of negative and positive effects on photosynthesis, bacterial production and other marine biological processes (Vincent and Belzile, 2003). The effects on either process from reduced sea ice cover in the Arctic are still unknown.

Compared to lower latitude shelves, photodegradation of CDOM in the Mackenzie Shelf waters is restricted to just a few months in the polar summer, yet several forcing factors make the overall effect of

* Corresponding author. Tel.: +1 919 515 0382; fax: +1 919 515 7802.
E-mail address: chris_osburn@ncsu.edu (C.L. Osburn).

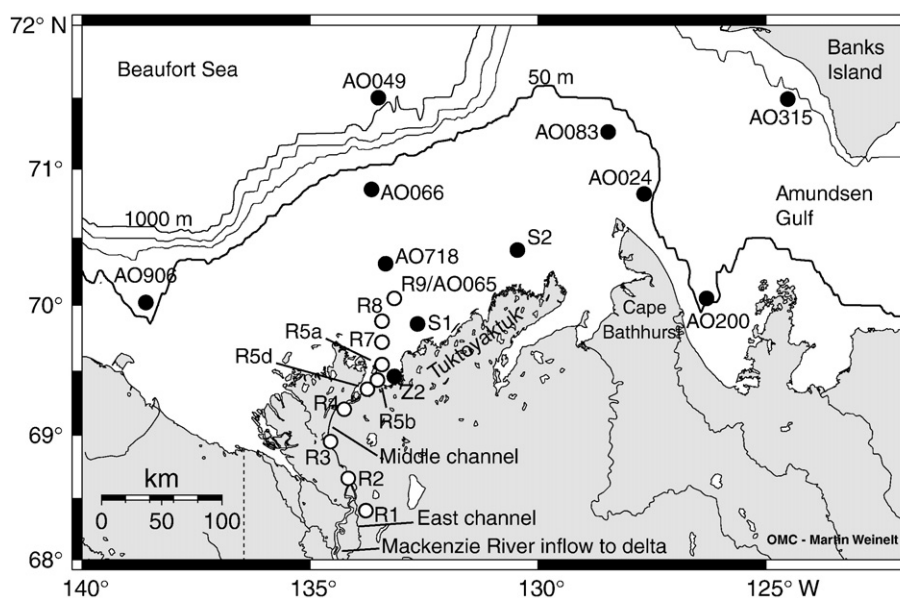


Fig. 1. Sampling locations on the Mackenzie shelf; the inlet to the Mackenzie River delta and the East and Middle channels where sampling occurred are indicated (map produced at <http://www.aquarius.ifm-geomar.de/>). Open circles indicate stations collected during the ARDEX cruise in July–August 2004. Closed circles indicate stations collected during the CASES2002 and CASES2003–2004 expeditions.

photodegradation unclear. First, the low sun angle at high latitudes results in a relatively lower sunlight intensity on surface waters than at lower latitudes. Second, sea ice cover and the large particulate load of the Mackenzie River reduce sunlight penetration in surface waters. However, sunlight is nearly continuous during the short polar summer, so a substantial cumulative dose is possible. Third, the changing quantity of Mackenzie River CDOM released after break-up and during free ice conditions (Emmertson et al., 2008) indicates that CDOM reactivity may change as day length increases during the polar summer. Finally, oceanographic features such as ice shoal (stamuhki) development on fast ice (Emmertson et al., 2008; Galand et al., 2008) and the anticyclonic Beaufort gyre can retain river water in the coastal zone for long periods of time (Macdonald et al., 1999). In combination, these latter factors may enable exposure of Mackenzie River CDOM to substantial photochemical processing in the very surface waters.

Bélanger et al. (2006) estimated that nearly 6% of Mackenzie River DOC can be photomineralized in the Beaufort Sea in ice free periods, yet CDOM photoreactivity varies in shelf waters and after exposure to sunlight. For example, Johannessen and Miller (2001) demonstrated that apparent quantum yields (AQY) for CDOM photomineralization can change significantly inshore to offshore, and with prior sunlight exposure. Similarly, Osburn et al. (2001) showed that AQY for CDOM photobleaching were significantly lower in the surface mixed layer of temperate lakes than at depth during summer stratification. In this report, we calculated AQY for CDOM photobleaching and photomineralization to study the CDOM photoreactivity of a series of surface samples collected from the Mackenzie River, its freshwater–saltwater transition zone through a small estuary, and across the Mackenzie Shelf to the Amundsen Gulf. We hypothesized that the most photoreactive CDOM occurs on the shelf after break-up, but that a long residence time might reduce its photoreactivity. We then used the AQY to predict photodegradation in the surface waters of the Mackenzie Shelf during the polar summer and compared our results to previous work in this region.

2. Methods

2.1. Sample collection and processing

Surface water samplings of the Mackenzie River and the Beaufort Sea were performed in October 2002 and from October 2003 to June

2004 during the Canada Arctic Shelf Exchange Study expeditions (CASES; details at <http://cases.quebec-ocean.ca>). During 28 July to 02 August 2004, a satellite expedition (Arctic River Delta Experiment; ARDEX, see Vincent and Pedrós-Alió, 2008) was conducted for this study. In the CASES expeditions, samples were collected from two sites (R1 and R2) upriver via helicopter, coastal sites near the river mouth, and along the shelf edge into the Beaufort Sea aboard the icebreaker CCGS *Pierre Radisson* (2002) or the icebreaker CCGS *Amundsen* (2003–2004). For the ARDEX expedition, river sampling aboard the CCGS *Nahidik* was conducted through out the delta and the river's East and Middle Channels, and along a transect extending from the river mouth at Kugmallit Bay to about 100 km offshore at station R9, which coincided with CASES station AO065 (Fig. 1).

Shipboard samples were collected from Niskin bottles affixed to a rosette or from surface grabs in cleaned plastic buckets. Riverbank sampling by helicopter involved collecting 20 L of surface water by manually filling cleaned polyethylene carboys by immersion below the water surface. Each collection procedure involved triple rinsing a container with surface water before filling with sample. All samples were vacuum-filtered through 0.2 μm filters into acid-cleaned polycarbonate and polyethylene bottles and stored in the dark at 4 °C until transport back to Washington, DC. Aliquots for DOC concentration were acidified with 85% H_3PO_4 and stored in the dark at 4 °C. CDOM absorption and fluorescence measurements were made within 3 days of receipt.

DOC concentration was measured on an OI Analytical 1010 TOC analyzer. Acidified samples were sparged for 10–15 min with UHP He to remove inorganic C. Osburn and St-Jean (2007) have modified this persulfate-based TOC analyzer to measure seawater DOC. Samples were calibrated against 0, 83, 208, 416, and 833 μM DOC standard solutions made from potassium hydrogen phthalate. The average relative standard deviation on this system was 3%, corresponding to an average standard error of 6 μM C. The limit of detection is 12–15 μM C.

CDOM absorption was measured in the laboratory on a Shimadzu UV1601 spectrophotometer in 5- or 10-cm pathlength cuvettes against 18 μM MilliQ laboratory water and converted to absorption coefficients as follows:

$$a_{\lambda} = A_{(\lambda)} \times 2.303 / l, \quad (1)$$

where λ = wavelength, A is the absorbance from the spectrophotometer, and l is the pathlength in meters. Absorption spectra were modeled from 280 to 650 nm using a nonlinear fitting technique based on the exponential decrease of CDOM absorption with increasing wavelength:

$$a_{\lambda} = a_{375} \times e^{S \times (375 - \lambda)} + K, \quad (2)$$

where λ is wavelength, S is the spectral slope coefficient, and K is a fitting parameter (Stedmon and Markager, 2003). K was only used for fitting and represented <5% of the value of a_{375} ; it was not included in the computation of absorption coefficients. CDOM absorption was quantified at 330 nm and the rate of decrease in absorption with wavelength was summarized with S .

CDOM synchronous fluorescence (SF) was measured on a Shimadzu RF-5301PC spectrofluorometer. For SF, a 14 nm offset ($\Delta\lambda$) between excitation and emission was used (Belzile et al., 2002). Excitation and emission internal calibrations were performed on the fluorometer according to manufacturer specifications and the calibrated results were reported in Raman units (nm^{-1}) by normalization to the water Raman fluorescence (Nieke et al., 1997). All data manipulations and statistical analyses were performed in the MATLAB (Mathworks, Inc., Natick, MA) computing environment using the Statistics and Curve Fitting Toolboxes.

2.2. Photodegradation experimental protocols

Filtered water samples were poured into quartz vessels in triplicate and closed with ground-glass stoppers to exclude air bubbles, then placed in a water bath on the rooftop of the Chemistry Building at the Naval Research Laboratory in Washington, DC and exposed to sunlight directly for a period of three days (O'Sullivan et al., 2005; Osburn et al., 2001). Triplicate samples wrapped in foil served as dark controls and were incubated simultaneously with exposed samples. A similar photodegradation experiment was run shipboard during the ARDEX expedition, in which Mackenzie River water was exposed to ambient sunlight from 31 July 2004 to 01 August 2004. This experiment allowed us to compare results from experiments conducted at mid-latitudes with an experiment conducted in the Arctic. In one experiment using Mackenzie River CDOM from October 2002, bottles were removed from exposure and analyzed after 24, 48, and 72 h of sunlight exposure to establish rates of photodegradation. In a separate 3-day experiment with Mackenzie River CDOM from October 2002, the sunlight exposure was modified by placing several Schott long-pass optical cutoff filters above triplicate samples (Osburn et al., 2001). We performed these experiments at various times between April and June 2003 and between April and October 2004. While the duration of exposure was consistent, CDOM samples were exposed to variable amounts of sunlight irradiance (within 20%).

Sunlight incident on the samples for each experiment was quantified with a Biospherical Instrument PUV-501b radiometer, which measures irradiance at 305, 320, 340, and 380 nm in $\text{mW cm}^{-2} \text{nm}^{-1}$, averaged over 60 second intervals. For each experiment, a cumulative dose at each wavelength was calculated in units of $\text{mol photons m}^{-2} \text{nm}^{-1}$ and used as input to a model that estimates the solar spectrum from 280 to 500 nm (Osburn et al., 2001). The dose absorbed by the sample (I_a) in $\text{mol photons m}^{-3} \text{nm}^{-1}$ for the experiment was calculated as:

$$I_{a,\lambda} = I_{0,\lambda} \times \left(1 - e^{-a_{\text{geo},\lambda} \times L}\right), \quad (3)$$

where $I_{0,\lambda}$ is the incident dose in $\text{mol photons m}^{-2} \text{nm}^{-1}$, λ is the wavelength in nm, $a_{\text{geo},\lambda}$ is the geometric average of the initial and final absorption, and L is the pathlength in meters. The geometric average estimates the nonlinear change in absorption that occurs from solar exposure (Osburn et al., 2001).

Because molar concentrations of CDOM are unknown, as are the molar concentrations of exact DOC compounds that are photomineralized, "apparent" QY (AQY) were subsequently calculated:

$$\text{AQY}_{\text{effect}} = \frac{\Delta\text{effect}}{\text{mol photons absorbed}} \quad (4)$$

The ' Δeffect ' was either the change in absorption (CDOM photobleaching, AQY_{ble}) or DOC concentration (CDOM photomineralization, AQY_{min}), and the mol photons absorbed was the integrated I_a from 280 to 500 nm. CDOM photoreactivity was defined as AQY calculated for absorption loss at 330 nm (photobleaching) and AQY calculated for DOC loss (photomineralization). Because AQY normalizes photochemical processes to the sunlight absorption required to initiate them, samples having widely variable CDOM concentrations exposed to different doses of sunlight may be compared for the common photobleaching or photomineralization effect.

Apparent quantum yield spectra (effect per nm) both for photobleaching and for photomineralization were computed from the cutoff filter experiment using CDOM from the Mackenzie River and from the Mackenzie shelf (station AO066, from O'Sullivan et al., 2005). The formula used to describe CDOM photobleaching or photomineralization from each cutoff filter experiment was modified from Johannessen and Miller (2001) and Hu et al. (2002),

$$\eta_{\text{effect}} = \int (I_{a,\lambda} \times \phi_{\text{effect},\lambda} \times d\lambda). \quad (5)$$

η_{effect} is either the photobleaching at 330 nm ($\text{m}^{-1} \text{m}^{-3}$) or the mineralization of DOC (mol C m^{-3}), $I_{a,\lambda}$ is the mol photons absorbed from Eq. (4), and ϕ_{effect} is the AQY spectrum for photobleaching or photomineralization (280 to 500 nm). The photomineralization of DOC calculations most closely matched the production of DIC measured and modeled by Bélanger et al. (2006) and Johannessen and Miller (2001) and may be used with irradiance spectra to predict photodegradation. A best fit of predicted results to measured results was performed using nonlinear optimization (the 'nlinfit' procedure in Matlab®). The functional form of ϕ_{effect} was chosen based on Johannessen and Miller (2001):

$$\phi_{\text{effect}} = e^{-(m_1 + m_2(\lambda - 290))}. \quad (6)$$

The m_1 and m_2 parameters are varied to minimize the difference between predicted and measured values.

3. Results

3.1. Variability in CDOM properties of the Mackenzie River and across the Mackenzie Shelf

CDOM and DOC concentrations of the Mackenzie River showed substantial variation among seasons, with the highest values occurring just after peak discharge in June and lowest values in August (Table 1). In late autumn (October 2002), before freeze-up, CDOM values were intermediate, yet DOC concentrations were highest in the data set. DOC concentration in the Mackenzie River had decreased by ~30% from June to August. CDOM synchronous fluorescence at 375 nm excitation (SF_{375}) showed a similar trend and was highly correlated with CDOM absorption (Pearson's $r=0.96$). Plots of CDOM and DOC properties versus salinity were used to assess mixing between river water and the Beaufort Sea. CDOM was generally conservative with salinity through the Mackenzie River, estuary, and out onto the Mackenzie shelf (Table 2). The highest spectral slope coefficient (S) values were measured offshore, and the Mackenzie River itself had a range of S values from $\sim 17.5 \mu\text{m}^{-1}$ in spring to $19.30 \mu\text{m}^{-1}$ in late summer. Both a_{330} and SF_{375} had high

Table 1

Characteristics of stations sampled along the ARDEX and CASES cruise transects from 2002 to 2004. Stations are separated into river, estuary, shelf, and gulf regions, based on geographical locations. n/a = data not available.

Station	Region	Cruise	Season	Year	Latitude (°N)	Longitude (°W)	Maximum depth (m)	Sampling depth (m)	Salinity	Temperature (°C)	a_{330} (m^{-1})	DOC (μM)	S (μm^{-1})	SF ₃₇₅ ($nm^{-1} \times 10^{-3}$)
R1	River	CASES	Autumn	2002	68.38	132.25	shore	0	0.1	3.90	10.15	576	18.58	28.94
R2	River	CASES	Autumn	2002	68.60	134.20	shore	0	0.1	3.90	10.22	512	18.62	28.17
R3	River	CASES	Spring	2004	68.88	134.57	30	0	0.1	17.10	13.30	508	17.50	39.96
R3	River	ARDEX	Summer	2004	68.88	134.57	30	0	0.1	17.10	5.51	339	19.22	18.44
R4	River	ARDEX	Summer	2004	68.20	134.23	19	0	0.4	17.87	5.84	312	19.39	19.30
Z2	Estuary	CASES	Autumn	2002	69.55	133.42	n/a	0	25.4	-0.54	1.32	133	20.05	5.81
S1	Estuary	CASES	Spring	2004	69.86	132.64	n/a	0	1.0	1.20	10.66	453	17.18	35.02
R5d	Estuary	ARDEX	Summer	2004	69.36	133.74	4	0	1.6	14.39	5.51	267	19.21	20.73
R5b	Estuary	ARDEX	Summer	2004	69.43	133.52	4	0	4.5	14.01	5.19	250	19.32	19.76
R5a	Estuary	ARDEX	Summer	2004	69.46	133.15	3	0	8.2	12.21	4.86	231	19.34	17.98
R7	Estuary	ARDEX	Summer	2004	69.72	133.42	7	0	21.8	21.81	2.68	160	20.05	9.21
AO066	Shelf	CASES	Autumn	2002	70.85	133.65	78	2	20.3	-0.61	1.96	166	20.48	7.14
AO083	Shelf	CASES	Autumn	2002	71.26	128.46	55	2	25.2	-1.34	1.23	120	20.41	5.06
AO049	Shelf	CASES	Autumn	2002	71.50	133.50	1000	2	26.3	-0.67	0.58	110	25.46	2.47
AO065	Shelf	CASES	Autumn	2002	70.15	133.15	43	2	26.7	-0.32	0.78	97	24.46	2.56
AO718	Shelf	CASES	Autumn	2003	70.31	133.34	30	2	21.1	n/a	1.24	144	22.05	4.53
AO906	Shelf	CASES	Spring	2004	70.02	138.60	270	2	15.8	8.06	4.51	229	18.17	13.86
R9	Shelf	ARDEX	Summer	2004	70.05	133.42	32	0	25.2	9.23	1.46	142	19.91	4.90
R8	Shelf	ARDEX	Summer	2004	69.88	133.42	16	0	27.0	7.35	1.34	136	20.77	4.28
S2	Shelf	CASES	Spring	2004	70.41	130.45	n/a	0	28.9	-1.2	0.98	109	20.97	4.36
R9	Shelf	ARDEX	Summer	2004	70.05	133.42	32	21	32.5	-1.36	0.73	102	19.56	3.53
AO024	Gulf	CASES	Autumn	2002	70.82	127.67	150	4	22.8	0.12	1.52	126	20.78	5.42
AO315	Gulf	CASES	Autumn	2003	71.49	124.52	211	0	27.2	-1.39	0.77	109	21.29	3.44
AO200	Gulf	CASES	Winter	2003	70.05	126.30	230	0	29.9	-1.68	0.73	113	18.28	4.16
AO200	Gulf	CASES	Winter	2003	70.05	126.30	230	0	30.6	-1.68	0.81	70	19.27	2.89
AO200	Gulf	CASES	Winter	2004	70.05	126.30	230	0	30.8	-1.68	0.61	108	19.27	2.92
AO200	Gulf	CASES	Spring	2004	70.05	126.30	230	12	30.8	-1.68	0.65	78	22.44	2.98

correlation coefficients when compared to DOC concentration (a_{330} : $r = 0.97$; SF₃₇₅: $r = 0.95$).

Synchronous fluorescence (SF) spectra revealed two distinct peaks at 350 and 375 nm excitation (SF₃₅₀ and SF₃₇₅, respectively) for the Mackenzie River. The latter peak at 375 nm was minimal or absent from surface waters sampled offshore (Fig. 2), so SF₃₇₅ was chosen to represent the Mackenzie River CDOM. SF₃₇₅ was still measurable at these sites (generally $<6 \times 10^{-3} nm^{-1}$) and was relatively conservative with salinity (Table 2).

3.2. Photobleaching of CDOM

Sunlight exposure decreased the absorption coefficient at 330 nm and the synchronous fluorescence intensity at 375 nm, so Δa_{330} and ΔSF_{375} were negative (Table 3). The absorption coefficients of dark controls for each CDOM sample exposed to sunlight did not change significantly during experiments when compared to initial values ($p > 0.05$). The relative standard deviation of photobleaching measurements on triplicate samples exposed to sunlight was $<5\%$ of the averaged value.

Samples having the highest CDOM and DOC values also had the highest Δa_{330} and ΔDOC values and mol photons m^{-2} absorbed (Table 3). For example, the correlation between Δa_{330} and a_{330} was 0.96 ($p < 0.05$, $n = 27$). Thus, the river and estuary samples exhibited more photodegradation than did the shelf and gulf samples. Moreover, the June and October samples exhibited more photodegradation than did the August samples. The smallest Δa_{330} ($-0.05 m^{-1}$) was measured for AO200, a sample collected while the icebreaker was

frozen in Franklin Bay, and representing the highest salinity sample (~ 31) furthest from the Mackenzie River. CDOM photodegradation did not increase the S values for all samples, and there was no significant correlation between ΔS and S. Similar to CDOM absorption, SF₃₇₅ values decreased with light exposure and the loss of SF₃₇₅ was correlated to the initial SF₃₇₅ ($r = -0.95$, $p < 0.05$, $n = 27$).

Differential SF spectra (final minus initial) for the river and estuary samples were distinct from the shelf and gulf samples (Fig. 3). Though a loss of SF₃₅₀ was observed for all samples, the magnitude of SF loss for the river and estuary samples was nearly 10 times that of the shelf and gulf samples. Further, the river and estuary samples exhibited extensive bleaching at excitation wavelengths > 350 nm that was not observed in the shelf and gulf results. This signal was most distinct for the river samples having the strongest initial CDOM absorption and initial SF (Table 1).

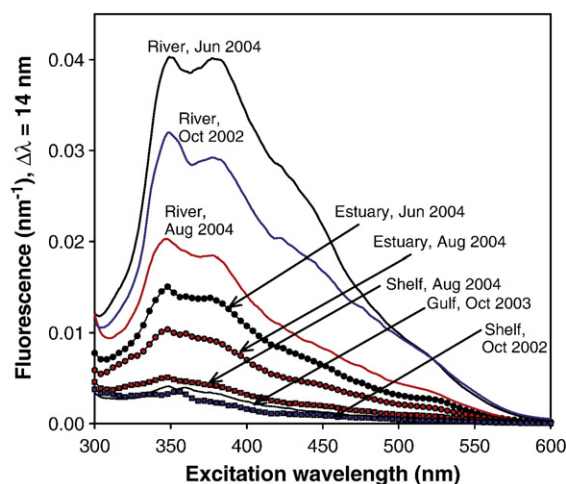


Fig. 2. The change in synchronous fluorescence spectra of samples collected in the Mackenzie River and across the Mackenzie Shelf to the Amundsen Gulf. The offset from the excitation wavelength was 14 nm.

Table 2

Linear regression analysis results for CDOM absorption, fluorescence, and DOC concentration trends with salinity.

Regression equation	r^2	p	N
SF ₃₇₅ = 26.54 - 0.82 × salinity	0.84	<0.001	27
DOC = 403.12 - 10.70 × salinity	0.80	<0.001	27
a_{330} = 8.37 - 0.27 × salinity	0.79	<0.001	27

Table 3
Results of photodegradation experiments on the optical and chemical properties of CDOM from the Mackenzie River across the Mackenzie Shelf.

Station	Region	Season	Salinity	Δa_{330} (m^{-1})	ΔS (μm^{-1})	ΔSF_{375} ($\text{nm}^{-1} \times 10^{-3}$)	ΔDOC ($\mu\text{M} \pm \text{S.D.}$)	Dose ($\text{mol photons m}^{-2}$)
R3	River	Spring	0.1	-5.85	3.92	-26.94	-159 (8)	56.690
S1	Estuary	Spring	1.0	-3.90	2.92	-23.52	-144 (22)	51.050
AO906	Shelf	Spring	15.8	-1.54	2.11	-7.53	-123 (12)	22.283
S2	Shelf	Spring	28.9	-0.26	0.83	-1.72	-22 (10)	4.810
AO200	Gulf	Spring	30.8	-0.23	3.75	-1.00	n.d.	2.600
R3	River	Summer	0.1	-1.61	0.70	-16.75	n.d.	19.450
R4	River	Summer	0.4	-1.58	0.70	-10.18	-28 (3)	20.850
R5d	Estuary	Summer	1.6	-1.24	0.71	-9.99	-24 (2)	20.300
R5b	Estuary	Summer	4.5	-1.25	0.90	-10.45	-23 (2)	18.820
R5a	Estuary	Summer	8.2	-1.24	0.52	-8.34	-17 (1)	17.570
R7	Estuary	Summer	21.8	-0.68	-0.89	-3.68	-12 (1)	9.898
R9	Shelf	Summer	25.2	-0.27	-0.01	-1.62	n.d.	6.620
R8	Shelf	Summer	27.0	-0.31	-0.64	-1.08	-15 (1)	4.890
R9	Shelf	Summer	32.5	-0.19	-1.07	-1.23	n.d.	2.572
R1	River	Autumn	0.1	-2.71	2.32	-27.78	-110 (6)	47.220
R2	River	Autumn	0.1	-2.82	2.72	-26.05	-116 (6)	47.590
AO066	Shelf	Autumn	20.3	-0.78	1.17	-2.09	-61 (4)	12.650
AO718	Shelf	Autumn	21.1	-0.50	1.79	-0.74	-12 (6)	3.370
AO024	Gulf	Autumn	22.8	-0.17	0.91	-2.73	n.d.	4.110
AO083	Shelf	Autumn	25.2	-0.22	1.54	-3.61	-17 (2)	3.180
Z2	Estuary	Autumn	25.4	-0.20	1.19	-4.71	n.d.	4.140
AO049	Shelf	Autumn	26.3	-0.25	2.16	-1.30	-49 (3)	2.481
AO065	Shelf	Autumn	26.7	-0.12	1.53	-0.61	n.d.	10.400
AO315	Gulf	Autumn	27.2	-0.27	0.53	-1.34	-11 (3)	3.010
AO200	Gulf	Winter	29.9	-0.05	1.61	-2.02	n.d.	2.450
AO200	Gulf	Winter	30.6	-0.15	-0.60	-2.18	n.d.	3.242
AO200	Gulf	Winter	30.8	-0.13	0.52	-0.97	-13 (6)	3.430

The results are grouped by season then by salinity. For ΔDOC , S.D. = standard deviation and n.d. = not determined.

3.3. Photomineralization of CDOM

A decrease in DOC concentration (ΔDOC) was measured only on 18 of the 27 samples studied during photodegradation experiments (sample loss prohibited measurement on the remaining nine samples). Similar to photobleaching results, the magnitude of CDOM photomineralization was greatest for the river and estuary samples and smallest for the shelf and gulf samples (Table 3). For the Mackenzie River, most photomineralization ($>100 \mu\text{M}$ DOC lost) occurred in samples collected in June 2004 and October 2002. Estuary samples from June 2004 (Stations S1 and AO906) also had losses of DOC $>100 \mu\text{M}$. The overall range was 20–30% DOC photomineralized. By contrast, the less absorptive river and estuary samples from August 2004 showed ~10% loss of DOC from photomineralization.

After 19 h of near-continuous sunlight exposure of Mackenzie River water in the shipboard experiment during ARDEX, its DOC decreased by $37 \pm 5 \mu\text{M}$, even with moderate cloud cover. The light dose for this experiment was $7.79 \times 10^{-1} \text{ mol photons m}^{-2}$, equivalent to the 3-day exposures for the experiments conducted in September 2004 in Washington, DC. The resulting photomineralization was about 12% of the initial DOC concentration. This amount of photomineralization was comparable to the loss of DOC measured when Station R4 was exposed to sunlight for three days in Washington, DC (Table 3).

3.4. Kinetic effects of photodegradation on Mackenzie River CDOM

Roughly half of the total photobleaching at a_{330} occurred in the first 24 h of exposure for Mackenzie River CDOM (Table 4). Incremental bleaching between time points were significant based on a one-way ANOVA ($p < 0.01$). Similar results were obtained for DOC concentration. An exponential fit to these results was used to compute a half-life of 3.7 days for a_{330} and a half-life of 4.8 days for DOC concentration. Coincident with the loss of CDOM absorption was an increase in S values from 18.56 to $20.86 \mu\text{m}^{-1}$ after 72 h of sunlight exposure, also significant ($p < 0.01$), and indicating a larger decrease in longwave UV-A and blue absorption relative to shortwave UV-B absorption. Again, most of the increase in S value (46%) occurred after the first 24 h of exposure. Similar to the CDOM absorption

results, ~50% of the photobleaching of SF intensity both at 350 nm and at 375 nm excitation occurred in the first 24 h, though after 72 h, the SF_{350} peak was photobleached the most (Fig. 4A).

3.5. Spectral effects of photodegradation on Mackenzie River CDOM

As progressively more UV radiation was removed from incident irradiance by the cutoff filters (which transmit between 0.2 and 1% at wavelengths below the 50% cutoff), Δa_{330} and ΔDOC were reduced (Table 4). There was no significant difference in photobleaching between the 'no filter' and the 305 nm cutoff treatment, but the photomineralization results were significantly different. Removing most wavelengths below 350 nm with the 357 nm cutoff filter produced about half of the photodegradation that occurred in full sunlight.

In the 395 nm cutoff treatment, $<1\%$ of the incident UV radiation (280 to 380 nm) was transmitted. This degree of removal produced 27% of the photobleaching and 20% of the photomineralization that occurred in 'no filter' treatment. Differences between adjacent filter treatments were significant only in the middle of the treatment group (one-way ANOVA; $p > 0.05$; $df = 7$; F statistic = 292.93).

Modifying the spectral quality of sunlight produced more complex responses in S value and in SF. The maximum change in S values for Mackenzie River CDOM occurred in the 314 and 335 nm cutoff treatments, which were not significantly different ($p > 0.05$; Table 4). Inclusion of more short wave radiation in the 305 nm cutoff and 'no filter' treatments decreased ΔS . About 30% of the maximum increase in S value occurred in the 395 nm cutoff filter treatment.

Removal of shortwave UV radiation produced greater photobleaching at SF_{375} than at SF_{350} (Fig. 4B). SF_{350} remained a recognizable peak, even in the 335 nm treatment where SF_{375} lacked any peak shape. The decreases in SF_{350} and SF_{375} were equivalent in the 314 nm cutoff filter and in full sunlight treatments.

Though removal of UV radiation with cutoff filters diminished photomineralization, similar degrees of photomineralization were reached after 24 h of full sunlight exposure and after 72 h in the 357 nm cutoff filter experiment. Thus, irradiation environments in

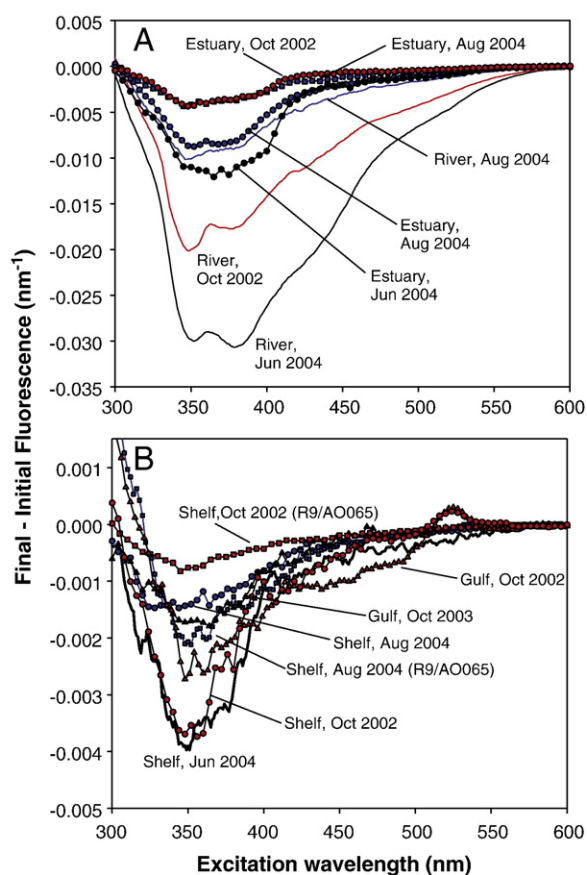


Fig. 3. Differential spectra (final–initial values) show the effect of photobleaching on synchronous fluorescence for A) the river and estuary samples and B) the shelf samples.

which most of the spectral composition was blue and longwave regions of the solar spectrum (e.g., >380 nm) could photomineralize Mackenzie River CDOM, albeit at slower rates when short wave UV radiation was excluded.

3.6. Apparent quantum yield calculations for CDOM photoreactivity

For experiments where no cutoff filters were used, apparent quantum yields (AQY) for photobleaching at 330 nm (AQY_{ble}) and for photomineralization of DOC to DIC (AQY_{min}), were calculated

to compare photodegradation results amongst samples absorbing different amounts of sunlight (Table 3). Though AQY_{ble} remained relatively constant ($0.080 \text{ m}^{-1} (\text{mol photon}^{-1})$) from river to the shelf, AQY_{ble} varied from 0.010 to $0.140 \text{ m}^{-1} (\text{mol photon}^{-1})$ in autumn and winter at salinities above 25 (Fig. 5A). AQY_{min} values calculated for the Mackenzie River were 50% greater in spring 2004 and in autumn 2002 than in summer 2004, but in general AQY_{min} values higher at salinities above 25 (Fig. 5B). No effect of salinity was found on AQY_{ble} when results from all seasons were pooled together, whereas for AQY_{min} , a weak, yet significant, linear relationship was found:

$$AQY_{min} \left(\times 10^{-3} \text{ mol C } (\text{mol photon}^{-1}) \right) = 1.855 + 0.0683 \times \text{Salinity} \\ r^2 = 0.39, n = 18, p < 0.01. \quad (7)$$

The cutoff filter results for Mackenzie River CDOM allowed us to compute apparent quantum yield spectra (ϕ) and compare those results to results of a similar cutoff filter experiment using CDOM from station AO066 (as reported in O'Sullivan et al., 2005). Each ϕ for a specific response (photobleaching, ϕ_{ble} , or photomineralization, ϕ_{min}), was a function that produced spectral weights from 280 to 500 nm. The function used to model the spectral response (Eq. (6)) produced r^2 values >0.9 as an estimate of how well the model fit the data. For each response, each model's coefficients were significantly different between the river and shelf sources (Table 5). The ϕ_{ble} for the Mackenzie River showed higher wavelength dependence toward the UV-B region than did the ϕ_{ble} for Mackenzie Shelf and was greater in magnitude (Fig. 5C). Conversely, ϕ_{min} was greater for the Mackenzie Shelf than for the river, and no difference in wavelength dependence was apparent (Fig. 5D).

4. Discussion

4.1. Synchronous fluorescence patterns

Fluorescence was a sensitive indicator of CDOM source on the Mackenzie Shelf that showed the dominance of the Mackenzie River signal and its loss over the shelf. The SF_{375} peak observed in the river samples was also reported by Retamal et al. (2007) for the Mackenzie River. While the decrease in SF_{375} appeared conservative along the salinity gradient of the shelf much like other CDOM properties (Table 2), it was also clear that duration and spectral distribution of sunlight irradiance could produce variable changes in SF spectra of the Mackenzie River CDOM (Fig. 4). To evaluate this effect, the Pearson's

Table 4

Results of photodegradation experiments to determine kinetic rates of, and to evaluate spectral effects on, both CDOM absorption and DOC concentration of Mackenzie River water.

Experimental design	Time elapsed (hr)	Cutoff filter (50% transmission wavelength)	Initial a_{330} (m^{-1})	Δa_{330} (m^{-1})	Initial S (μm^{-1})	ΔS (μm^{-1})	Initial DOC (μM)	ΔDOC (μM)
Kinetic experiment, April 2003	0		10.22		18.62		512	
	13	No filter		-1.35 (0.04)		1.06 (0.04)		-56 (6)
	26	No filter		-2.25 (0.03)		1.85 (0.10)		-84 (6)
	39	No filter		-2.74 (0.04)		2.31 (0.12)		-110 (6)
Filter experiment, June 2003	0		10.15		18.58		576	
	45	No filter		-2.86 (0.23)		2.67 (0.22)		-116 (6)
	45	305 nm		-2.84 (0.03)		2.77 (0.07)		-99 (2)
	45	314 nm		-2.53 (0.07)		3.14 (0.03)		-98 (2)
	45	335 nm		-2.06 (0.02)		3.04 (0.09)		-85 (1)
	45	357 nm		-1.54 (0.03)		2.54 (0.02)		-57 (1)
	45	375 nm		-1.04 (0.06)		1.55 (0.07)		-39 (1)
	45	389 nm		-0.83 (0.02)		1.28 (0.09)		-28 (4)
	45	395 nm		-0.77 (0.02)		1.02 (0.02)		-23 (2)

'No filter' means exposure to full sunlight. Values in parentheses are standard deviations to 1σ .

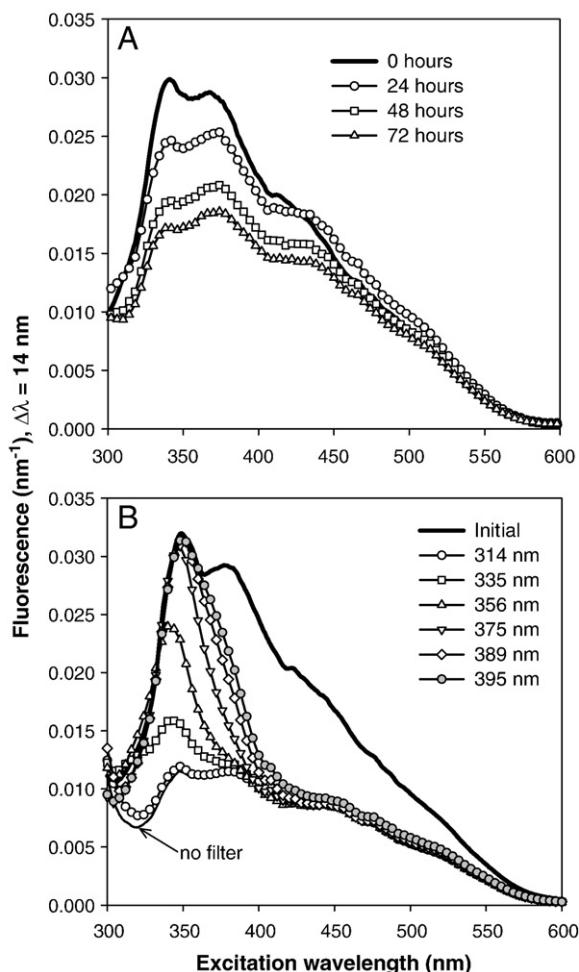


Fig. 4. The effects of photobleaching on synchronous fluorescence as a function of A) duration of exposure, and B) removal of incident irradiance through the use of optical cutoff filters.

correlation coefficient (r) between each river water SF spectrum and the several estuary, shelf, and gulf water SF spectra was calculated before and after photobleaching as an index of spectral similarity (Fig. 6). The Pearson's r values were mostly >0.80 , indicating a high degree of similarity in the fluorescent signatures. The highest correlations (approaching 1.0) occurred for the river stations and the estuary stations. After photobleaching, modest increases occurred in the Pearson's r values between most shelf and gulf waters (Fig. 6), yet photobleaching typically decreased the Pearson's r for the estuary stations. Thus, photobleaching apparently made Mackenzie River CDOM more closely resemble Beaufort Sea CDOM. Using only CDOM properties to distinguish water mass mixing may be complicated in coastal regions where photodegradation occurs.

While the changes to SF spectra were generally similar among the filter treatments, the 335 nm cutoff filter treatment produced a Mackenzie River SF spectrum more highly correlated to the shelf and gulf samples than did the 305 nm cutoff filter treatment, and certainly higher than the non-photobleached river water (Fig. 6A). No change in Pearson's r value was seen when the photobleached river SF spectra were correlated to CDOM samples taken at middle (15 m) and bottom (21 m) depths for shelf station R9 in August 2004 (data not shown). Thus the effect does appear to be restricted to surface waters. These results imply that primarily longwave UV-A irradiance is producing the SF spectral changes on the shelf and the Amundsen Gulf, consistent with a light environment where UV-B attenuation is high due to CDOM and to particles (Retamal et al., 2008).

Supporting this assertion are differences to the change in the S value of Mackenzie River CDOM when the spectral quality of irradiance is modified. Selective removal of shortwave UV radiation (<330 nm) in the 335 nm cutoff filter treatment resulted in proportionally more longwave bleaching and produced a larger increase in S value than did the 305 nm cutoff filter treatment. Based on these results, S values of the Mackenzie River should increase from 18.6 to 21.7 μm^{-1} with extensive photobleaching. This closely matches the distribution of S values measured for the region (Table 1) and emphasizes the importance of the Mackenzie River for the carbon cycle of this shelf.

4.2. Photoreactivity of CDOM

Similar to the CDOM photodegradation results reported by Amon and Meon (2004) for the Yenisei and Ob estuaries, exposure of Mackenzie River water to sunlight during the ARDEX cruise photomineralized about 40 μM DOC after 19 h. This rate of photomineralization produced a DOC half life of 4.3 days, very similar to the 4.8 day half life calculated from exposure of Mackenzie River CDOM at mid-latitude sunlight (Section 3.4). The sky conditions during the ARDEX exposure experiment were partly cloudy, which is common for polar summers in this region. Thus the estimate of photomineralization is conservative, but very likely representative of an upper limit on potential CDOM photomineralization in surface waters of the coastal Beaufort Sea. Based on the photomineralization results from the rate experiment (Table 4), 40 μM DOC represents 57% of the potential photomineralization that could occur in Mackenzie River CDOM at lower latitudes.

With respect to salinity, the photoreactivity of CDOM bleaching appeared uncoupled to the photoreactivity of DOC mineralization. While the loss of CDOM absorption and the loss of fluorescence were each highly correlated to the loss of DOC (Fig. 7), the apparent quantum yields for CDOM photobleaching were not correlated to those for DOC photomineralization (Pearson's $r = 0.03$, $N = 18$). The uncoupling between the photobleaching of CDOM absorption and the photomineralization of DOC could be explained by the sunlight exposure history of Mackenzie River water on the shelf. Osburn et al. (2001) found that AQY values decreased in the surface waters of stratified lakes after sunlight exposure and it is reasonable to assume that surface waters on the Mackenzie Shelf remain stratified during the polar summer. Only one of the AQY_{ble} values on the Mackenzie Shelf was substantially greater than the range of Mackenzie River AQY_{ble}; the remaining values were equal to, or less than, the range of AQY_{ble} for the river. Given that the polar summer is more or less continuous illumination (factoring in cloud cover), prior light exposure could have caused the decreased AQY_{ble} measured for the shelf. We cannot, however, discount the addition of less reactive CDOM to the region, perhaps from sea ice melt or from primary production (Bélanger et al., 2006). Johannessen and Miller (2001) suggested that bleaching may be required before mineralization in strongly absorbing CDOM, such as that in the Mackenzie River. The lack of change or decrease in AQY_{ble} with salinity, compared with the increase of AQY_{min} with salinity supports this assertion.

Our photoreactivity results were similar to those for coastal waters as reported by Johannessen and Miller (2001). However, the photoreactivity values presented here are different from those reported by Bélanger et al. (2006) who studied the same region yet used a different equation to compute ϕ_{min} . To compare the photomineralization results from this study with these and other publications, we multiplied each ϕ_{min} by a midday irradiance spectrum modeled by a radiative transfer program for the Mackenzie Shelf (in $\text{mol photon}^{-1} \text{s}^{-1}$), and computed a 'photochemical response' akin to Johannessen and Miller (2001) and Bélanger et al. (2006). The response was $36.94 \times 10^{-6} \text{ mol C (mol photons}^{-1})$ for the river and $42.87 \times 10^{-6} \text{ mol C (mol photons}^{-1})$ for the shelf. These responses compare favorably to the inshore (salinity <31) response of $30.4 \times 10^{-6} \text{ mol C (mol photons}^{-1})$ reported in

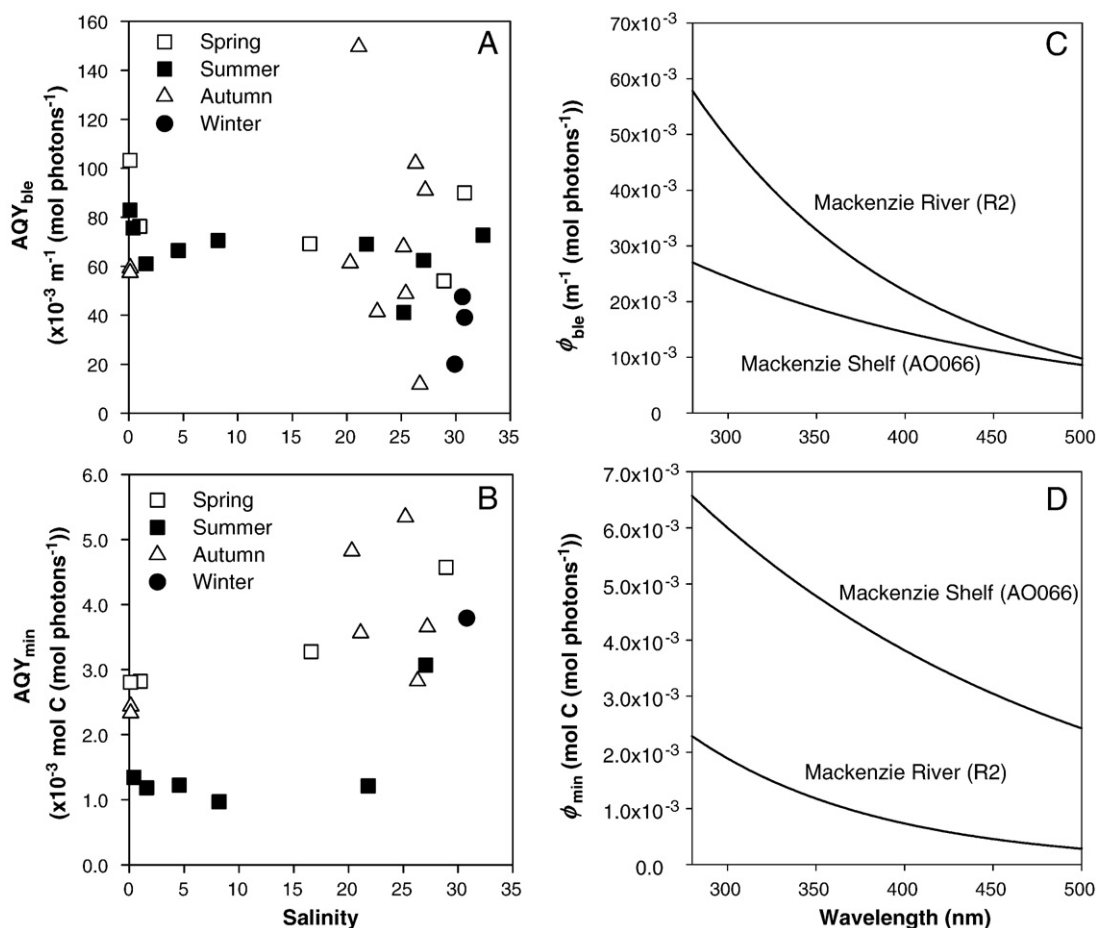


Fig. 5. The results of AQY calculations for A) CDOM photobleaching at 330 nm and B) DOC photomineralization, plotted as a function of salinity. The wavelength dependence of C) photobleaching and D) photomineralization for the Mackenzie River and the Mackenzie Shelf are also shown.

Johannessen and Miller (2001) and were only slightly higher than the values reported in Bélanger et al. (2006) for the same region. Vähätalo et al. (2000) computed similar AQY spectra for photomineralization of humic lake CDOM and reported a response of 25.9×10^{-6} mol C (mol photons) $^{-1}$, slightly lower than that computed here.

The dependence of CDOM photoreactivity on absorbed dose across the Mackenzie Shelf and into the Amundsen Gulf is important in terms of climate change to the Arctic region. If climate warming alters the Mackenzie River basin and delta hydrology to mobilize more terrestrial DOM as previously suggested (Guo et al., 2007; Emmerton et al., 2008), then our AQYs for the June 2004 samples, collected just after peak discharge, suggest an increase in the distribution of this photoreactive material across the Mackenzie shelf. Station R3 and S1, for example, had the largest CDOM absorption and DOC concentrations and also the largest mol photons absorbed. Subsequently, just a few days' light exposure mineralized 130 μ g C in our photodegradation experiments (the quartz bottle volume was 0.073 L). While photobleaching could produce the changes between spring and summer in the optical and chemical properties of the Mackenzie River observed here, it is unlikely that the river water CDOM itself was photodegraded to any extent within the Mackenzie Delta.

4.3. Modeling of CDOM photodegradation

On the Mackenzie Shelf, the complex structure of the mixed layer sustains stratification of the river plume (Carmack and Macdonald, 2002), in which high light attenuation from particles occurs (Retamal et al., 2008). Del Vecchio and Blough (2002) have demonstrated that the depth of photodegradation (pd) relative to the vertical mixing

depth (vmd) will control the extent of observable CDOM photodegradation, because an extensive mixing depth can resupply unaltered CDOM to surface waters. Thus the ratio of $pd:vmd$ will be especially critical for photoreactions on the Mackenzie Shelf.

Light attenuation values (K_d) from the ARDEX cruise were reported for the Mackenzie River and the Mackenzie Shelf by Retamal et al. (2008). Using their values, we computed 1% irradiance depths for 330 nm ($z_{1\%}$). At station R3 in August 2004, $z_{1\%}$ was 0.12 m, increasing to 0.5 m in the estuary (station R5a) and to 1.84 m at station R8. While the goal of this study was not to produce a functioning water column model of photodegradation, estimation of photodegradation over limited periods for two stations on the Mackenzie Shelf (R7 and R8) was possible. Stations S1 and AO906 were used to include photodegradation estimates for the more photoreactive spring CDOM. The attenuation data from Retamal et al. (2008) showed that these stations

Table 5

Spectral weighting function equations as the apparent quantum yields (ϕ) for CDOM photobleaching at 330 nm (ϕ_{ble}) and CDOM photomineralization (ϕ_{min}).

CDOM source (station)	Response	m_1	m_2	r^2
Mackenzie River (R2)	ϕ_{ble}	0.555 ± 0.150	-0.0081 ± 0.0027	0.99
	ϕ_{min}	6.18 ± 0.26	0.0095 ± 0.0031	0.98
Mackenzie shelf (AO066)	ϕ_{ble}	3.66 ± 0.44	0.0052 ± 0.0026	0.92
	ϕ_{min}	5.07 ± 0.15	0.0045 ± 0.002	0.9

Two model parameters, m_1 and m_2 , from Eq. (6) are reported. The r^2 value is an estimate of goodness-of-fit from the nonlinear optimization procedure.

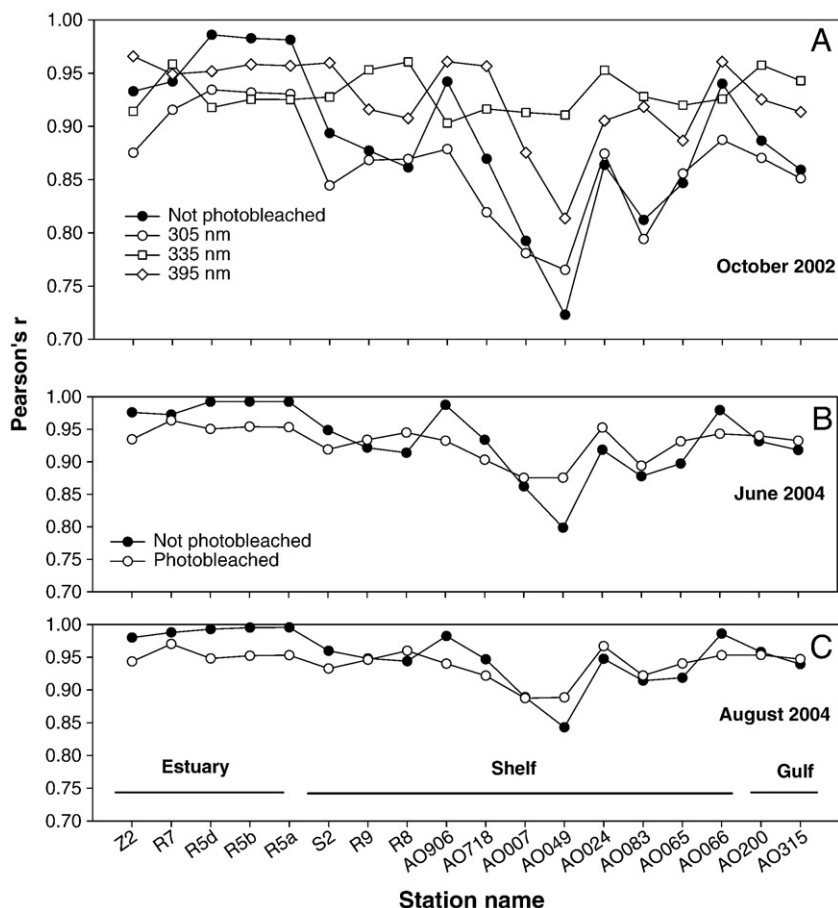


Fig. 6. The results of the Pearson's r correlation between Mackenzie River CDOM collected in A) 2002, B) June 2004, and C) October 2004, and estuary, shelf, or gulf CDOM. The higher r values indicated very similar SF spectra.

had pd of at least 1 m, which was 20% of the vmd at R7 and 14% of the vmd at R8.

Based on the $z_{1\%}$ values, 0.05 m was chosen as a conservative estimate of the effective depth over which to model CDOM photobleaching and photomineralization using ϕ_{ble} and ϕ_{min} . Note that this depth would reduce the $pd:vmd$ ratio by another 50%, so these results are strictly sea surface estimates. An exponential fit to Retamal et al.'s K_d values was used to estimate spectral K_d from 280 to 500 nm. Combining these attenuation values with our CDOM data, and integrating over the depth range, the following formula was used to compute each photodegradation effect:

$$\text{Loss} = \int \int E_0(\lambda, z) \times \phi_{min}(\lambda) \times a(\lambda) / K_d(\lambda) d\lambda dz. \quad (8)$$

Here, 'Loss' is either photobleaching or photomineralization, $\lambda = 280$ to 500 nm, and $z = 0$ to 0.05 m, at 0.01 m intervals. The river quantum yield spectra were used for station R7 (the outermost reach of the estuary) and station S1. The shelf quantum yield spectra were used for stations R8 and AO906.

Our model calculations resulted in decrease of a_{330} and DOC concentration over 36 h of exposure during August 2004 at 70°N, 134°W (Table 6). The decreases in a_{330} and DOC concentration were lower than the results of the photodegradation experiments on the same samples (cf. Table 3). The discrepancy underscores the reduction in photodegradation resulting from high light attenuation in a water column. Note also that the observed amount of photodegradation would be reduced further by vertical upwelling of particles and unreacted CDOM from advection and eddy diffusion within the surface mixing layer.

Despite the constraints of low sun angle and water column light attenuation with depth, it is remarkable that the modeled CDOM photobleaching indicated an average loss of 7% relative to initial values, whereas the modeled CDOM photomineralization indicated <1% decrease relative to initial values. Thus CDOM optical signatures (such as SF) could be about 7% less than would be predicted from conservative mixing alone due to this non-conservative process (Stedmon and Markager, 2003). The net effect of photodegradation on the Mackenzie Shelf ecosystem is unknown, but clearly photobleaching can play a role in making surface water more transparent to sunlight, especially in the damaging UV-B region. In fact, the balance of increased UV exposure of organisms from ice-free conditions and photobleaching to the probable increase in attenuation from larger delivery of riverine CDOM to Arctic shelf regions remains unknown (Gibson et al., 2000).

These preliminary estimates demonstrate that photodegradation of CDOM, while certainly occurring on the very surface layers of the Arctic Ocean, does not remove substantial amounts of the riverine DOM that fluxes through the Arctic. With substantial photodegradation, plots of DOC vs. salinity should reveal concavity, which they do not (Whitehouse et al., 1989; Guéguen et al., 2005; Bélanger et al., 2006; Emmerton et al., 2008). These results are consistent with studies elsewhere in the coastal Arctic Ocean that have suggested a negligible role for DOM photodegradation (Dittmar and Kattner, 2003; Amon and Meon 2004).

In terms of Arctic Ocean shelf biogeochemistry, Bélanger et al. (2006) estimated areal mass fluxes of DIC by photodegradation in the range of 3–5 mg C m⁻² d⁻¹ for the Mackenzie Shelf in late July. In similar units, our estimated values of DOC photomineralization ranged between 1–2 mg C m⁻² d⁻¹ for late July 2004. In June 2004, the

values were much higher, from 3 to 10 mg C m⁻² d⁻¹. These values are still small, however, relative to microbial degradation rates of DOC, which continue throughout the year at an estimated average value of 73 mg C m⁻² d⁻¹ (Garneau et al., 2008). In comparison to the DIC photoproduction estimates by Bélanger et al. (2006), our estimates for CDOM photomineralization, constrained to the top 0.5 m, are very similar. It is encouraging that measurements of CDOM photomineralization from two different methodologies have produced comparable results. Moreover, the results underscore the photoreactivity of CDOM in Arctic rivers (Amon and Meon, 2004) and that DIC photoproduction is restricted to the sea surface layer (<0.5 m) due to a low *pd:vmd* ratio.

In conclusion, our observations of CDOM optical and chemical properties combined with photochemical modeling provide additional estimates of the photoreactivity for a major source of C to the Arctic Ocean. The Mackenzie River clearly was the dominant source of CDOM to the coastal Beaufort Sea, yet we observed substantial seasonal variability in the amount of its CDOM, as did Guéguen et al. (2005), and in the photoreactivity of its CDOM. Estimates of the *pd:vmd* ratio calculated from data in Retamal et al. (2008) suggest only about the top meter would be subject to photodegradation on the Mackenzie Shelf, especially after ice-breakup and the subsequent major discharge of highly-attenuating, particle-rich river water across the shelf. Nevertheless, removal of most UV-B wavelengths from incident irradiation still produced about half of the photomineralization and photobleaching observed in full sunlight. The photochemical modeling shown here demonstrates that the CDOM in this region of the Beaufort Sea retains the photoreactivity of its Mackenzie River source with respect to photobleaching, yet its photoreactivity with

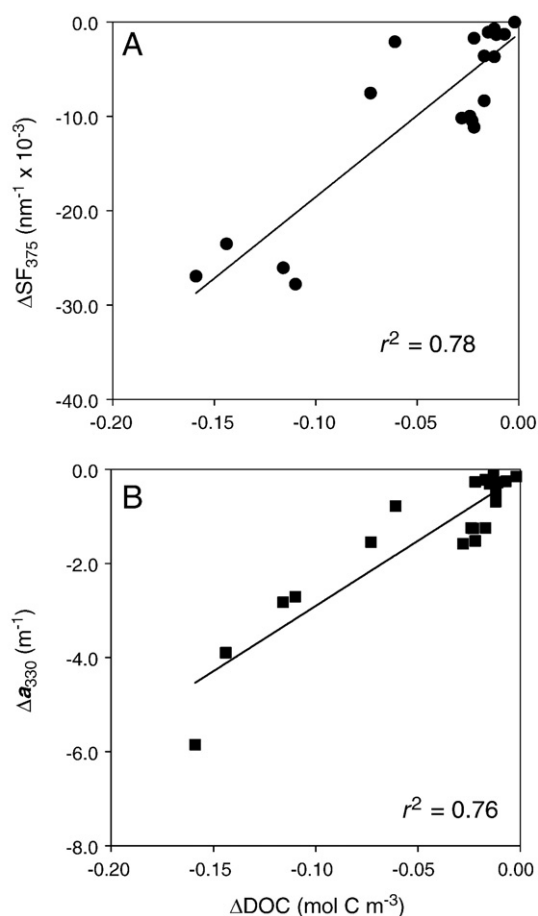


Fig. 7. The relationship between CDOM and DOC photodegradation, shown as A) the decrease in SF correlated to the decrease in DOC concentration and B) the loss of CDOM absorption at 330 nm correlated to the decrease in DOC concentration.

Table 6

CDOM photodegradation model results using the spectral AQY and incident solar irradiance measured during ARDEX (30 July to 01 August 2004).

Station	Predicted photobleaching at 330 nm (m ⁻¹ (m ⁻²))	% of initial value	Predicted photomineralization of DOC (mol C m ⁻²)	% of initial value
R7	0.40	15	0.13	<1
R8	0.03	2	0.16	<1
S1	0.78	7	0.31	<1
AO906	0.15	3	0.82	<1

See text for explanation of modeling parameters.

respect to photomineralization is enhanced somewhat at higher salinities. Prior photochemical and microbial aging of Mackenzie River CDOM may explain this disconnect in photoreactivity between CDOM optical and chemical properties. The potential for river water to remain in the region for periods of 7–10 years through entrainment as sea ice in the Beaufort Gyre (Macdonald et al., 1999) suggests this possibility as a contribution of sea ice melt to surface waters of the Mackenzie Shelf (Macdonald et al., 1989). Further research in this area should couple models of CDOM photodegradation to water mass circulation to improve estimates of this carbon removal process during the Arctic summer.

Acknowledgements

The comments of two anonymous reviewers greatly improved this manuscript. We thank the captains and crews of the CCGS *Pierre Radisson*, *Amundsen*, and *Nahidik* for their support and professionalism, Polar Shelf Canada for their excellent helicopter logistics support, and our colleagues in the CASES and ARDEX programs. Kevin Johnson and Tom Boyd of the US Naval Research Laboratory provided valuable comments regarding statistical analyses. This research was funded by Office of Naval Research Grant N0001403WX20946 to CLO and grants from the Natural Sciences and Engineering Research Council NSERC) and Canada Research Chair to WFV.

References

- Amon, R.M.W., Meon, B., 2004. The biogeochemistry of dissolved organic matter and nutrients in two large Arctic estuaries and potential implications for our understanding of the Arctic Ocean system. *Mar. Chem.* 92, 311–330.
- Bélanger, S., Xie, H., Krotkov, N., Larouche, P., Vincent, W.F., Babin, M., 2006. Photomineralization of terrigenous dissolved organic matter in Arctic coastal waters from 1979 to 2003: interannual variability and implications of climate change. *Glob. Biogeochem. Cycles* 20, GB4005. doi:10.1029/2006GB002708.
- Belzile, C., Gibson, J.A.E., Vincent, W.F., 2002. Colored dissolved organic matter and dissolved organic carbon exclusion from lake ice: implications for irradiance transmission and carbon cycling. *Limnol. Oceanogr.* 47, 1283–1293.
- Carmack, E.C., Macdonald, R.W., 2002. Oceanography of the Canadian Shelf of the Beaufort Sea: a setting for marine life. *Arctic* 55, 29–45.
- Del Vecchio, R., Blough, N.V., 2002. Photobleaching of chromophoric dissolved organic matter in natural waters: kinetics and modeling. *Mar. Chem.* 78, 231–253.
- Dittmar, T., Kattner, G., 2003. The biogeochemistry of the river and shelf ecosystem of the Arctic Ocean: a review. *Mar. Chem.* 83, 103–120.
- Dixon, R.K., Brown, S., Houghton, R.A., Solomon, A.M., Trexler, M.C., Wisniewski, J., 1994. Carbon pools and flux of global forest ecosystems. *Science* 263, 185–190.
- Droppo, I.G., Jeffries, D., Jaskot, C., Backus, S., 1998. The prevalence of freshwater flocculation in cold regions: a case study from the Mackenzie River Delta, Northwest Territories, Canada. *Arctic* 51, 155–164.
- Emmertson, C.A., Lesack, L.F.W., Vincent, W.F., 2008. Mackenzie River nutrient delivery to the Arctic Ocean and effects of the Mackenzie Delta during open water conditions. *Glob. Biogeochem. Cycles* 22, GB1024. doi:10.1029/2006GB002856.
- Galand, P.E., Lovejoy, C., Pouliot, J., Garneau, M.-E., Vincent, W.F., 2008. Microbial community diversity and heterotrophic production in a coastal Arctic ecosystem: a stamukhi lake and its source waters. *Limnol. Oceanogr.* 53, 813–823.
- Garneau, M.-E., Roy, S., Lovejoy, C., Gratton, Y., Vincent, W.F., 2008. Seasonal dynamics of bacterial biomass and production in a coastal Arctic ecosystem: Franklin Bay, western Canadian Arctic. *J. Geophys. Res.* 113, C07S91.
- Gibson, J.A.E., Vincent, W.F., Nieke, B., Pienitz, R., 2000. Control of biological exposure to UV radiation in the Arctic Ocean: comparison of the roles of ozone and riverine dissolved organic matter. *Arctic* 53, 372–382.
- Guéguen, C., Guo, L., Tanaka, N., 2005. Distributions and characteristics of colored dissolved organic matter in the Western Arctic Ocean. *Cont. Shelf Res.* 25, 1195–1207.

- Guo, L., Ping, C.-L., Macdonald, R.W., 2007. Mobilization pathways of organic carbon from permafrost to arctic rivers in a changing climate. *Geophys. Res. Lett.* 34, L13603. doi:10.1029/2007GL030689.
- Hu, C., Muller-Karger, F.E., Zepp, R.G., 2002. Absorbance, absorption coefficient, and apparent quantum yield: a comment on common ambiguity in the use of these optical concepts. *Limnol. Oceanogr.* 47, 1261–1267.
- Johannessen, S.C., Miller, W.L., 2001. Quantum yield for the photochemical production of dissolved inorganic carbon in seawater. *Mar. Chem.* 76, 271–283.
- Macdonald, R.W., Carmack, E.C., McLaughlin, F.A., Iseki, K., Macdonald, D.M., O'Brien, M.C., 1989. Composition and modification of water masses in the Mackenzie shelf estuary. *J. Geophys. Res.* 94, 18,057–18,070.
- Macdonald, R.W., Solomon, S.M., Cranston, R.E., Welch, H.E., Yunker, M.B., Gobeil, C., 1998. A sediment and organic carbon budget for the Canadian Beaufort shelf. *Mar. Geol.* 144, 255–273.
- Macdonald, R.W., Carmack, E.C., McLaughlin, F.A., Falkner, K.K., Swift, J.H., 1999. Connections among ice, runoff and atmospheric forcing in the Beaufort Gyre. *Geophys. Res. Lett.* 26, 2223–2226.
- Mopper, K., Kieber, D.J., 2002. Photochemistry and the cycling of carbon, sulfur, nitrogen, and phosphorus. In: Hansell, D.A., Carlson, C.A. (Eds.), *Biogeochemistry of Marine Dissolved Organic Matter*. Academic Press, pp. 456–489.
- Nieke, B., Reuter, R., Heuermann, R., Wang, H., Babin, M., Therriault, J.C., 1997. Light absorption and fluorescence properties of chromophoric dissolved organic matter (CDOM), in the St Lawrence Estuary (Case 2 waters). *Cont. Shelf Res.* 17, 235–252.
- Oelke, C., Zhang, T.J., Serreze, M.C., 2004. Modeling evidence for recent warming of the Arctic soil thermal regime. *Geophys. Res. Lett.* 31. doi:10.1029/2003GL019300.
- Osburn, C.L., Morris, D.P., 2003. Photochemistry of chromophoric dissolved organic matter in natural waters. In: Hebling, E.W., Zagarese, H. (Eds.), *UV effects in Aquatic Organisms and Ecosystems*. The Royal Society of Chemistry, pp. 185–217.
- Osburn, C.L., St-Jean, G., 2007. The use of wet chemical oxidation with high-amplification isotope ratio mass spectrometry (WCO-IRMS) to measure stable isotope values of dissolved organic carbon in seawater. *Limnol. Oceanogr.: Methods* 5, 296–308.
- Osburn, C.L., Zagarese, H.E., Morris, D.P., Morris, Hargreaves, B.R., Cravero, W.E., 2001. Calculation of spectral weighting functions for the solar photobleaching of chromophoric dissolved organic matter in temperate lakes. *Limnol. Oceanogr.* 46, 1455–1467.
- O'Sullivan, D.W., Neale, P.J., Coffin, R.B., Boyd, T.J., Boyd, Osburn, C.L., 2005. Photochemical production of hydrogen peroxide and methylhydroperoxide in coastal waters. *Mar. Chem.* 97, 14–33.
- Peterson, B.J., McClelland, J., Curry, R., Holmes, R.M., Walsh, J.E., Aagaard, K., 2006. Trajectory shifts in the Arctic and subarctic freshwater cycle. *Science* 313, 1061–1066.
- Retamal, L., Vincent, W.F., Martineau, C., Osburn, C.L., 2007. Comparison of the optical properties of dissolved organic matter in two river-influenced coastal regions of the Canadian Arctic. *Estuar. Coast. Shelf Sci.* 72, 261–272.
- Retamal, L., Bonilla, S., Vincent, W.F., 2008. Optical gradients and phytoplankton production in the Mackenzie River and the coastal Beaufort Sea. *Polar Biol.* 31, 363–379.
- Stedmon, C.A., Markager, S., 2003. Behaviour of the optical properties of coloured dissolved organic matter under conservative mixing. *Estuar. Coast. Shelf Sci.* 57, 973–979.
- Vähätalo, A.V., Salonen, M.-S., Taalas, P., Salonen, K., 2000. Spectrum of the quantum yield for photochemical mineralization of dissolved organic carbon in a humic lake. *Limnol. Oceanogr.* 45, 664–676.
- Vincent, W.F., Belzile, C., 2003. Biological UV exposure in the polar oceans: Arctic–Antarctic comparisons. In: Huiskes, A.H.L., Gieskes, W.W.C., Rozema, J., Schorno, R.M.L., van der Vies, S.M., Wolff, W.J. (Eds.), *Antarctic Biology in a Global Context*. Backhuys Publishers, Leiden, The Netherlands, pp. 176–181.
- Vincent, W.F., Pedrós-Alió, C., 2008. Sea ice and life in a river-influenced arctic shelf ecosystem. *J. Mar. Syst.* 74. doi:10.1016/j.jmarsys.2008.03.003.
- Whitehouse, B.G., MacDonald, R.W., Iseki, K., Yunker, M.B., McLaughlin, F.A., 1989. Organic carbon and colloids in the Mackenzie river and Beaufort Sea. *Mar. Chem.* 26, 371–378.